

Original Article

C+F GFDM with Polynomial Model of HPA

Chhavi Sharma¹, Pankaj Sharma²

¹Department of ECE, M.J.P. Rohilkhand University Bareilly, Uttar Pradesh, India

²Department of ECE Rajshree Institute of Engineering and Management, Bareilly Uttar Pradesh, India

Received : 10 December 2021

Revised : 13 January 2022

Accepted : 25 January 2022

Published : 31 January 2022

Abstract - Generalized frequency division multiplexing (GFDM) is a new waveform modulation technique for next-generation wireless communication systems. However, it also has the drawback of a high peak-to-average power ratio (PAPR) like Orthogonal Frequency Division Multiplexing (OFDM). In the work, a simple clipping and filtering technique is proposed for PAPR reduction of the GFDM signal and the performance of the GFDM system with a polynomial model of HPA is shown for different performance metrics. The simulations are performed with a memoryless polynomial model of HPA. The BER performance of the proposed scheme is compared with orthogonal frequency division multiplexing (OFDM), which is a popular modulation scheme for 4th Generation wireless communication systems. It is clear from the results that PAPR and out-of-band leakage in the GFDM signal is reduced up to a large extent after applying the clipping and filtering method as compared to the OFDM signal maintaining almost equal BER performance.

Keywords - PSD, GFDM, OFDM, Polynomial.

1. Introduction

Intersymbol interference (ISI) is a major obstacle to the error-free transmission of wireless signals, which is caused due to multipath transmission in wireless communication. It becomes necessary to cancel the effect of ISI if the time delay between multipath is larger than the symbol duration. Two approaches are presented in the literature to reduce the effect of ISI. The first approach is to use equalizers which reduces the effect of ISI. However, this approach becomes complex if multipath distortion is larger in the system. The alternative approach is the adoption of multicarrier modulation (MCM), in which several low data rate bitstreams are transmitted parallel over sub-channels. OFDM is a popular multicarrier modulation scheme that is a strong waveform candidate for 4G wireless communication systems. It is popular due to many advantages like high spectral efficiency, high data rate, simple equalization methods etc. Besides many advantages, it suffers from two major drawbacks: high PAPR and high intercarrier interference (ICI). In the OFDM system, the signal is transmitted by converting the high data rate bit stream into many parallel bitstreams of low bit rates and then transmitted over subcarriers to reduce the effect of ISI. Maintaining orthogonality within subcarriers is a prime condition for OFDM transmission, and failing to achieve this condition results in high ICI. The other major drawback mentioned above is high PAPR which occurs in OFDM due to large peak power signals. These high peak power signals introduce additional inband and out-of-band (OOB) distortion in the system. These drawbacks make OFDM an unsuitable waveform candidate for future high-speed wireless systems. GFDM is currently introducing a multicarrier waveform modulation method, which overcomes the drawbacks of the OFDM multicarrier scheme [1].

Message symbols are transmitted in a block of frequency and time in GFDM, and then pulse shaping is performed on every subcarrier to control the out-of-band radiation and PAPR [2]. Although self, induced interference is generated in GFDM, which can be reduced with the help of self-interference cancellation techniques at the receiver end [3]. As mentioned above, the data transmitted in GFDM is in time and frequency manners, so fewer subcarriers are required to achieve spectral efficiency equivalent to OFDM. For the improvement in spectral efficiency of GFDM, the cyclic prefix is added to the entire block, but in the case of OFDM, it is added after every time slot, which makes OFDM more complex. These properties make GFDM a suitable choice for deployment in future communication systems.

Unlike other MCM systems, such as OFDM, GFDM also suffers from high PAPR [4], and the problem becomes severe when the high peak GFDM signal passes through the HPA. After passing through the high power amplifier (HPA), the high PAPR GFDM signal introduces additional interference into the system in the form of in-band and out-of-band leakage due to the nonlinear behaviour of HPA. It reduces the efficiency of the system and demands more battery life.

In literature, different PAPR reduction techniques are discussed, such as “coding, clipping, filtering, and Partial Transmit Sequence (PTS), Selective mapping (SLM), companding, Tone reservation (TR) and Tone Injection (TI)”, etc. [1]. Clipping is simple to operate among all these techniques and easy to implement. Clipping of a signal increases in-band and out-of-band noise in the signal; hence filtering of the signal is applied after clipping to reduce this noise. In this work, clipping and filtering (C+F) is used in an iterative manner which is quite a complex process for OFDM, but it is less complex in the case of GFDM as it requires a



lesser number of iterations to achieve the performance comparable to OFDM due to its pulse shaping property which reduces the out of band radiation.

The proposed work also presents the effect of nonlinearity distortion on Clipped and filtered Generalized Frequency Division Multiplexing (GFDM). Here the polynomial model of the power amplifier is considered. The analytical expression of power spectral density of clipped and filtered GFDM signal is also shown in the paper. Results from the simulation show that OOB radiation is reduced to a large extent after applying the filtering technique to the clipped GFDM system.

2. Proposed Scheme

Clipping is a technique in which a signal is deliberately clipped to reduce the peaks of the signal to achieve a low PAPR signal. In the present work, the C+F technique is applied for PAPR reduction of the GFDM signal. In this work, the effects of the proposed scheme on the PAPR performance of the GFDM system are analyzed and observed in the presence of a polynomial model of HPA. The baseband model of the GFDM transmitter/receiver is shown in Fig.1.

2.1. GFDM Modulator

GFDM is a block-based multicarrier scheme in which a block consists of K subcarriers that carry M sub-symbols. $N = KM$ are the total numbers of symbols in the GFDM system. The modulator of the GFDM system is shown in Fig.2.

The input data vector \vec{d} having N elements $\vec{d} = \{d_0, d_1, \dots, d_{N-1}\}$ are divided into K subcarriers and M sub-symbols as $\vec{d} = [d_{0,0}, \dots, d_{K-1,0} \quad d_{0,1}, \dots, d_{K-1,1} \dots d_{K-1,M-1}]^T$ hence total $N = KM$ data symbols are transmitted. In OFDM, the N input data samples are transmitted over N orthogonal subcarriers in a single time slot, i.e. $M=1$, whereas in GFDM, these samples are transmitted over K subcarriers in M time slots.

The transmission of GFDM is shown in Fig.2. In GFDM transmission, the signal is up-sampled first. Pulse shaping of the signal is performed, and the pulse-shaped signal is transmitted for carrier up-conversion. After applying these operations, the overall GFDM signal is obtained as in [7] and is given as:

$$x[n] = \sum_{k=0}^{K-1} \sum_{m=0}^{M-1} d_{k,m} \tilde{g}_{k,m}[n] \quad (1)$$

where, $n = 0, 1, \dots, N-1$ is the sample index, N is the number of samples per time slot, $m = 0, \dots, M-1$ and $k = 0, \dots, K-1$. The $d_{k,m}$ is a complex data symbol transmitted on the k^{th} subcarrier and m^{th} time slot and can be represented as

$$d = \begin{bmatrix} d_{(0,0)} \cdot \cdot \cdot d_{(0,M-1)} \\ \cdot \cdot \cdot \cdot \cdot \\ d_{(K-1,0)} \cdot \cdot \cdot d_{(K-1,M-1)} \end{bmatrix}$$

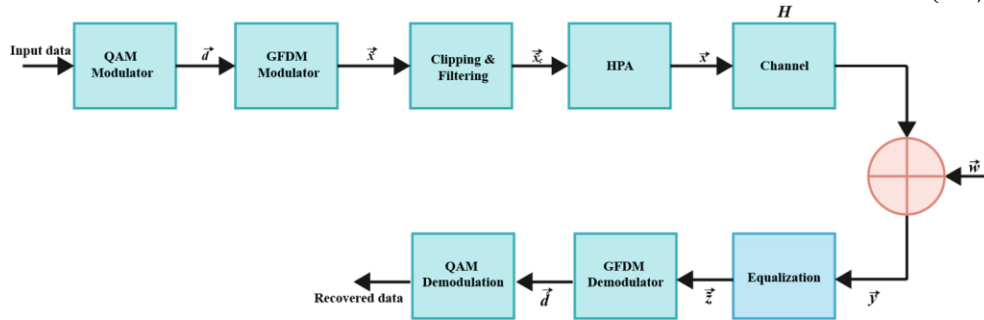


Fig. 1 C+F GFDM with a high-power amplifier

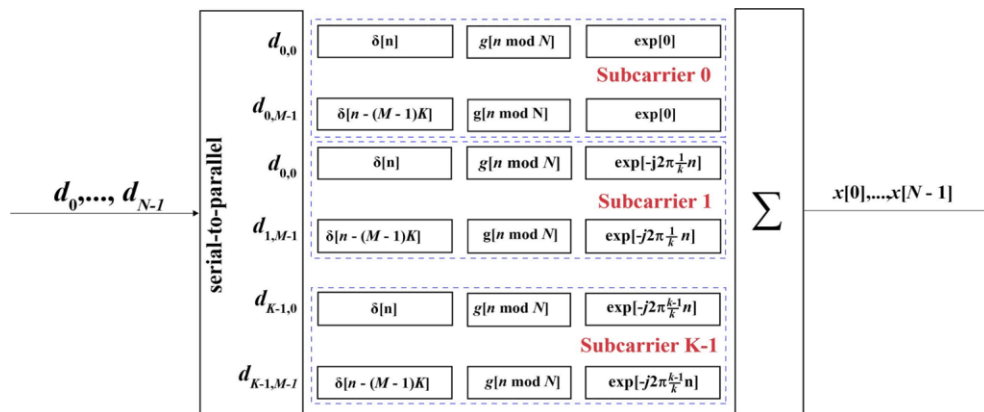


Fig. 2 GFDM modulator

and $\tilde{g}_{k,m}[n]$ is the time and frequency transformation of the circular pulse shaping filter of length N and is given as [4]

$$\tilde{g}_{k,m}[n] = g[(n - mK) \bmod N] w^{k,n} \quad (2)$$

where, $w^{k,n} = e^{-j2\pi kn/K}$

The GFDM transmitted signal $x[n]$ from (1) can also be expressed as a $KM \times KM$ modulation matrix":

$$x = Cd \quad (3)$$

where C represents GFDM signal processing steps and d is the data vector-matrix

$$[C] = g[(n - mK) \bmod N] e^{-j2\pi \frac{k}{K} n} \quad (4)$$

The demodulation of the GFDM signal is the reverse process of GFDM modulation, in which the received GFDM symbols are down-converted, applied to an inverse pulse shaping filter and then downsampling is performed to recover the original input data samples back.

2.2. Clipping and Filtering

The GFDM signal \vec{x} , after clipping, is expressed as [11]:

$$\vec{x}_c = \begin{cases} -A & \vec{x} \leq -A \\ \vec{x} & |\vec{x}| < A \\ A & \vec{x} \geq A \end{cases} \quad (5)$$

Where A denotes the clipping level. The clipping ratio CR can be defined as the ratio of clipping level to the RMS value ρ of \vec{x} , i.e.

$$CR = \frac{A}{\rho} \quad (6)$$

After the C+F operation, the GFDM signal is applied to HPA, and then the output of HPA is transmitted over a wireless fading channel after converting it to an RF signal. It is assumed that signal is received with perfect synchronization and channel estimation [6]. At the receiver of the GFDM system, the received signal \vec{y} is represented as:

$$\vec{y} = H \vec{x} + \vec{w} \quad (7)$$

Where H is the channel matrix, and \vec{w} is the AWGN noise? After equalization of the received signal \vec{y} , we get equalized signal \vec{z} as

$$\begin{aligned} \vec{z} &= H^{-1} \vec{y} \\ &= H^{-1} H \vec{x} + H^{-1} \vec{w} \end{aligned} \quad (8)$$

if $\vec{x} = \tilde{C} \vec{d}$, where \tilde{C} is the matrix after GFDM modulation with clipping and filtering and noise

$$\vec{w} = H^{-1} \vec{w}$$

$$\begin{aligned} \text{then equation (8) will be } \vec{z} &= H^{-1} H \tilde{C} \vec{d} + \vec{w} \\ &= \tilde{C} \vec{d} + \vec{w} \end{aligned} \quad (9)$$

After GFDM demodulation, the demodulated data \vec{d} is given by

$$\vec{d} = \tilde{B}_{ZF} \vec{z} \quad (10)$$

where, $\tilde{B}_{ZF} = \tilde{C}^{-1}$ is the zero-forcing receiver matrix that includes the down-conversion, circular convolution with receiver filter and downsampling of GFDM demodulation in one operation [9].

2.3. Power Amplifier

Here, the polynomial model of the power amplifier is considered to model the nonlinearity of the power amplifier. The output of a memoryless PA amplifier is represented in a polynomial model as in [12]:

$$p(t) = \sum_{i=0}^{2N_L+1} a_{2i+1} |x(t)|^{2i} x(t) \quad (11)$$

Where $p(t)$ is the power amplifier's output, $x(t)$ is the clipped and filtered GFDM signal and $2N_L + 1$ is the order of nonlinearity. Now, the autocorrelation function of PA calculates the psd of the power amplifier, which is as follows

$$R_{pp}(\tau) = E[p(t)p^*(t - \tau)] \quad (12)$$

$$= E \left[\sum_{i_1=0}^{2N_L+1} a_{2i_1+1} |x(t)|^{2i_1} x(t) \times \sum_{i_2=0}^{2N_L+1} a_{2i_2+1}^* |x(t - \tau)|^{2i_2} x^*(t - \tau) \right] \quad (13)$$

PSD of PA can be calculated by taking Fourier to transform as:

$$S_{pp}(f) = \int_{-\infty}^{\infty} R_{pp}(\tau) e^{-j2\pi f \tau} d\tau \quad (14)$$

3. Results and Discussion

16 QAM modulation scheme is used in the proposed GFDM system. In the simulation, 1000 GFDM modulated symbols are generated. Here, the zero-forcing detection method is applied to recover the GFDM signal. All the simulation results are obtained using the MATLAB tool. Simulation parameters are depicted in table 1. Here third-order polynomial model of PA is considered.

Table 1. Parameters for Simulation

Parameters	GFDM
“Subcarriers K	256
time slots M	4
Modulation Scheme	16QAM
Oversampling factor L	4
The roll-off factor of the RRC filter	0.3
High power amplifier	Memoryless polynomial model
Clipping ratio CR	1.2
Nonlinear coefficient (\mathbf{a}_1)	14.9740 + j0.0519
Nonlinear coefficient (\mathbf{a}_3)	23.0954 + j4.9680”

In Fig.3 (a) and Fig.3 (b), the PAPR reduction using clipping and filtering and PAPR reduction using only clipping technique are represented in the GFDM signal. Results show that at the same PAPR threshold level, PAPR is reduced by 3.9dB and 4.5 dB with CGFDM and C+F GFDM, respectively. Fig.4 shows the PSD comparison of OFDM and

GFDM, which verifies that GFDM is less out-of-band (OOB) radiation than OFDM. In Fig.5 and Fig.6, the performance of conventional GFDM and CGFDM is depicted. It is clear from the comparative results that after clipping operation to the GFDM signal, OOB leakage increases which can be further reduced after applying the filtering operation shown in Fig.5.

Further, bit error rate performances of OFDM and GFDM (with and without C+F) are depicted in Fig.7. It can be concluded from the results that conventional OFDM and GFDM systems have similar BER performance, but BER deviates slightly when the C+F scheme applied to the OFDM and GFDM systems.

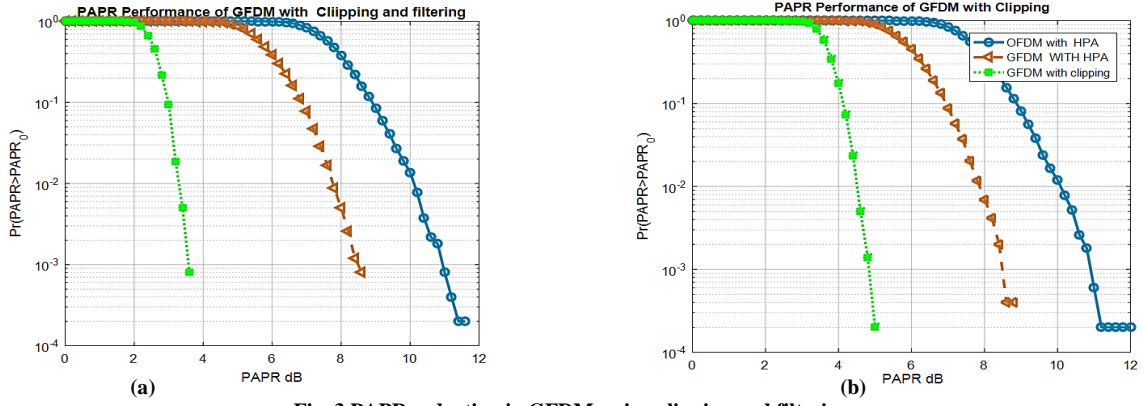


Fig. 3 PAPR reduction in GFDM using clipping and filtering

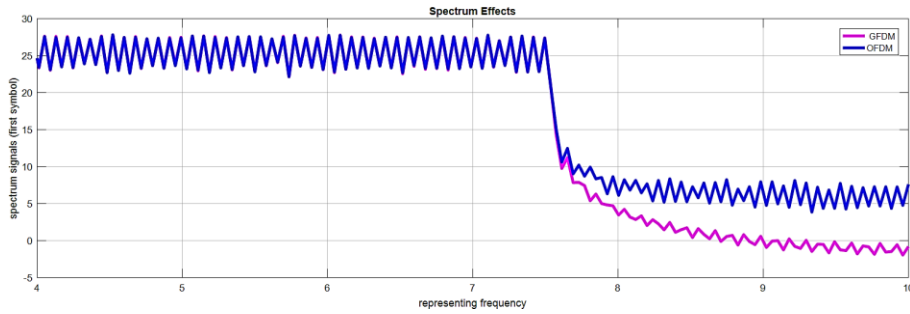


Fig. 4 OFDM and GFDM PSD comparison curves

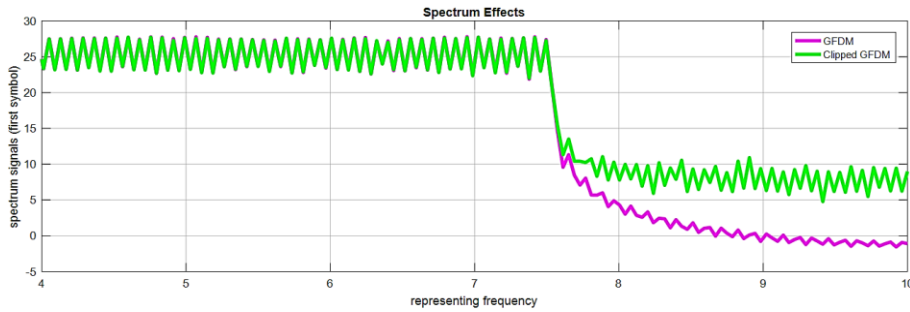


Fig. 5 Conventional GFDM and CGFDM PSD Comparison curves

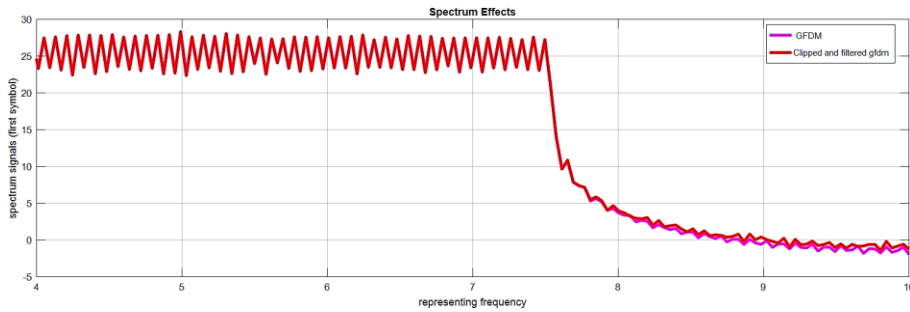


Fig. 6 PSD Comparison of C+F GFDM and conventional GFDM

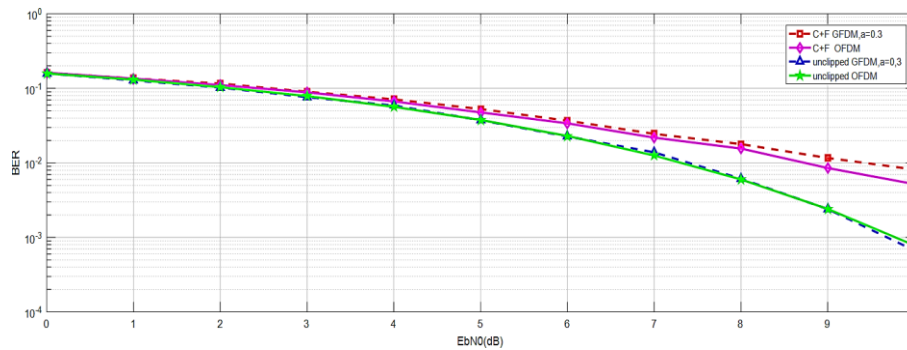


Fig. 7 BER performance comparison of C+F OFDM and C+F GFDM with conventional OFDM and GFDM

4. Conclusion

The work proposed here shows that PAPR and OOB leakage of the GFDM system is reduced to a large extent when

the filtering technique is applied to the clipped GFDM signal at the cost of small BER deviation, which can be further reduced by using successive interference cancellation method.

References

- [1] Tao Jiang, and Yiyan Wu, "An Overview: Peak-to-Average Power Ratio Reduction Techniques for OFDM Signals," *IEEE Transactions on Broadcasting*, vol. 54, no. 2, pp. 257-268, 2008. *Crossref*, <http://doi.org/10.1109/TBC.2008.915770>
- [2] Nicola Michailow et al., "Generalized Frequency Division Multiplexing for 5th Generation Cellular Networks," *IEEE Transactions on Communications*, vol. 62, no. 9, pp. 3045-3061, 2014. *Crossref*, <http://doi.org/10.1109/TCOMM.2014.2345566>
- [3] Nicola Michailow, and Gerhard Fettweis, "Low Peak-To-Average Power Ratio for Next-Generation Cellular Systems with Generalized Frequency Division Multiplexing," *International Symposium on Intelligent Signal Processing and Communications Systems (ISPACS)*, pp. 651-655, 2013. *Crossref*, <http://doi.org/10.1109/ISPACS.2013.6704629>
- [4] Paolo Banelli et al., "Modulation Formats and Waveforms for 5G Networks: Who Will Be the Heir of OFDM?: An Overview of Alternative Modulation Schemes for Improved Spectral Efficiency," *IEEE Signal Processing Magazine*, vol. 31, no. 6, pp. 80-93, 2014. *Crossref*, <http://doi.org/10.1109/MSP.2014.2337391>
- [5] Al'i Bulut Üçüncü, "Out-of-Band Radiation and CFO Immunity of Potential 5G Multicarrier Modulation Schemes," Master Thesis, The Graduate School of Natural and Applied Sciences of Middle East Technical University.
- [6] Luqing Wang, and C Tellambura, "A Simplified Clipping and Filtering Technique for PAR Reduction in OFDM Systems," *IEEE Signal Processing Letters*, vol. 12, no. 6, pp. 453-456, 2005. *Crossref*, <http://doi.org/10.1109/LSP.2005.847886>
- [7] Ari Endang Jayati, Wirawan, and Titiek Suryani, "Analysis of Nonlinear Distortion Effect based on Saleh Model in GFDM System," *IEEE International Conference on Communication, Network and Satellite (Comnesat)*, pp. 1-6, 2017. *Crossref*, <http://doi.org/10.1109/COMNETSAT.2017.8263564>
- [8] Gerhard Wunder et al., "5GNOW: Non-Orthogonal, Asynchronous Waveforms for Future Mobile Applications," *IEEE Communications Magazine*, vol. 52, no. 2, pp. 97-105, 2014. *Crossref*, <http://doi.org/10.1109/MCOM.2014.6736749>
- [9] Ivan Gaspar et al., "Frequency-Shift Offset-QAM for GFDM," *IEEE Communications Letters*, vol. 19, no. 8, pp. 1454-1457, 2015. *Crossref*, <http://doi.org/10.1109/LCOMM.2015.2445334>
- [10] AL'I BULUT ÜÇÜNCÜ, "Out-of-Band Radiation and CFO Immunity of Potential 5G Multicarrier Modulation Schemes," Middle East Technical University, 2015.
- [11] Luqing Wang, and C. Tellambura, "A Simplified Clipping and Filtering Technique for PAR Reduction in OFDM Systems," *IEEE Signal Processing Letters*, vol. 12, no. 6, pp. 453-456, 2006. *Crossref*, <http://doi.org/10.1109/LSP.2005.847886>
- [12] A. A. M. Saleh, "Frequency-Independent and Frequency-Dependent Nonlinear Models of TWT Amplifiers," *IEEE Transactions on Communications*, vol. 29, no. 11, pp. 1715-1720, 2005. *Crossref*, <http://doi.org/10.1109/TCOM.1981.1094911>
- [13] D. Dardari, V. Tralli, and A. Vaccari, "A Theoretical Characterization of Nonlinear Distortion Effects in OFDM Systems," *IEEE Transactions Communications*, vol. 48, no. 10, pp. 1755-1764, 2000. *Crossref*, <http://doi.org/10.1109/26.871400>
- [14] P. Banelli, and S. Cacopardi, "Theoretical Analysis and Performance of OFDM Signals in Nonlinear AWGN Channels," *IEEE Transactions on Communications*, vol. 48, no. 3, pp. 430-441, 2000. *Crossref*, <http://doi.org/10.1109/26.837046>